Spectroscopy 22 (2008) 63–82
DOI 10.3233/SPE-2008-0342
IOS Press

Structural dynamics of the Ca^{2+}-ATPase studied by time-resolved infrared spectroscopy

Andreas Barth
Department of Biochemistry and Biophysics, The Arrhenius Laboratories for Natural Sciences, Stockholm University, S-106 91 Stockholm, Sweden
Tel.: +46 8 162452; Fax: +46 8 155597; E-mail: Andreas.Barth@dbb.su.se

Abstract. This review discusses the contribution of time-resolved infrared spectroscopy to the understanding of the Ca^{2+} pump in the sarcoplasmic reticulum membrane of skeletal muscle cells (SERCA1a). The focus is on interactions of the substrate ATP with the ATPase and on the bond parameters of the phosphoenzyme phosphate group. Functional groups throughout the ATP molecule are important for stabilising the closed conformation of the ATP–ATPase complex and for fast phosphorylation of the ATPase. Dissociation of the reaction product ADP after phosphorylation leads to a more open average conformation of the enzyme and does not trigger the transition from the first phosphoenzyme Ca_2E1P to the second E2P. The P–O bond between phosphate and aspartyl moieties is weaker in Ca_2E1P and E2P than in acetyl phosphate in aqueous solution, which explains the high reactivity of the phosphoenzymes. This ground state property of the phosphoenzymes prepares for a phosphate transfer reaction with dissociative character.

Keywords: FTIR, SERCA, Ca^{2+} pump, structure, function

Abbreviations

AMPPCP – adenosine 5′-(β, γ-methylene)triphosphate;
TNP-AMP – 2′,3′-O-(2,4,6-trinitrophenyl)adenosine 5′-monophosphate

1. Ca^{2+}-ATPase

1.1. Overview

P-type ATPase are major players in primary active transport of ions across biological membranes as they consume ∼30% of the ATP produced in resting mammalian cells [1]. Their name derives from the fact that these enzymes become phosphorylated by ATP during the transport cycle. One of the best characterized members of this family is the Ca^{2+}-ATPase of the sarcoplasmic reticulum (SR) membrane from skeletal muscle (SERCA1a) [2] which serves as a model for the whole family of P-type ATPases [3].

The SR Ca^{2+}-ATPase transports Ca^{2+} from the cytoplasm of muscle cells into the SR lumen which relaxes a flexed muscle. Protons are countertransported in exchange for Ca^{2+}. Active transport of two

Ca^{2+} is fuelled by the free energy from the hydrolysis of one molecule of ATP which is used with up to 100% efficiency [4]. In contracting skeletal muscle cells, the Ca^{2+}-ATPase accounts for ∼20% of the ATP consumption [1].

1.2. Structure

The Ca^{2+}-ATPase consists of a single polypeptide of ∼1000 amino acids [5,6], which is the functional transport unit [7–11]. Determination of the amino acid sequence of the cardiac muscle Ca^{2+}-ATPase (SERCA2a, 997 residues) [5] and skeletal muscle Ca^{2+}-ATPase (SERCA1a, 1001 residues) [6] has enabled structural models that correctly predicted ten transmembrane helices and three cytoplasmic domains [5,6]. A first experimental glimpse of the three-dimensional structure has been provided by small angle X-ray scattering experiments of oriented samples [12,13], electron microscopy [14–16] and distance mapping by fluorescence energy transfer [17–19].

In 2000, Toyoshima and co-workers published the first structure at atomic resolution [20] shown on the left-hand side of Fig. 1(a). The Ca^{2+}-ATPase consists of a transmembrane domain (M) with ten transmembrane helices and three cytoplasmic domains: phosphorylation (P), nucleotide binding (N) and actuator (A) domain. The P domain contains the phosphorylation site Asp-351 and the N domain interacts with ATP. The two Ca^{2+} binding sites in the M domain are formed by main chain oxygens of residues Val-304 (Ca^{2+} binding site II), Ala-305 (site II), Ile-307 (site II), and side chain oxygens of Glu-309 (site II), Asn-768 (site I), Glu-771 (site I), Asn-796 (site II), Thr-799 (site I), Asp-800 (sites I and II), Glu-908 (site I) in transmembrane helices M4, M5, M6 and M8. The side chain ligands had been identified before by site directed mutagenesis [21,22].

1.3. Ca^{2+}-transport

The Ca^{2+}-ATPase reaction mechanism has been reviewed before [23–32] and is commonly described in terms of an E1/E2 scheme adapted from de Meis and Vianna [33]. However, the original interpretation of E1 and E2 as two main conformations of the enzyme with particular orientation and affinity of the Ca^{2+} binding sites had to be abandoned in the light of recent structural work. A simplified version of the reaction cycle is shown in Fig. 2.

Jencks and co-workers [34–37] have questioned the existence of reaction intermediates of the E1/E2 model. They have proposed a switch mechanism in which Ca^{2+} binding and Ca^{2+} release switch the reaction specificity of the phosphorylation site, whereas phosphorylation and dephosphorylation switch the accessibility and affinity of the Ca^{2+} sites [35]. This coupling between phosphorylation site and Ca^{2+} sites is necessary for efficient Ca^{2+} pumping and occurs over a distance of 50 Å. The scheme shown in Fig. 2 is a hybrid between the two views, it retains the E1/E2 notation for clarity, keeps the E1/E2 equilibrium of the Ca^{2+} free ATPase from the de Meis and Vianna scheme, but omits a state Ca_2E2P, which is usually not observed [36,38] but seems to be adopted in certain mutants [39,40] and when the Ca^{2+} free ATPase is inhibited by beryllium fluoride [41]. Figure 2 shows the minimum number of states that are adopted under physiological conditions.

The Ca^{2+}-free ATPase exists in a pH dependent equilibrium between an E2 form adopted at low pH and an E1 form at high pH [42,43]. It binds two cytosolic Ca^{2+} sequentially [44–47] to the two high affinity Ca^{2+} binding sites which releases two [43,48–52] or three [53] H^+ to the cytoplasm at pH 6. The models for Ca^{2+} binding differ as to whether each Ca^{2+} competes with one H^+ [43,49,50] or whether the protons have to be released before the first Ca^{2+} binds [48,50,52,53]. The latter is often interpreted

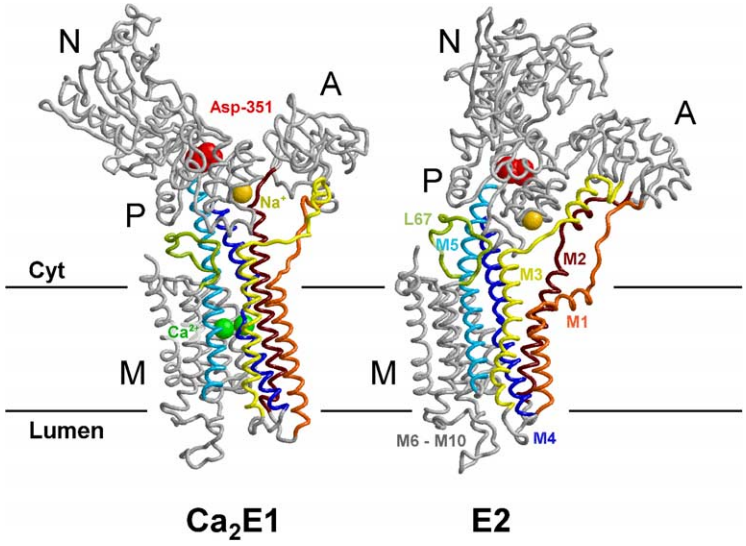

(a)

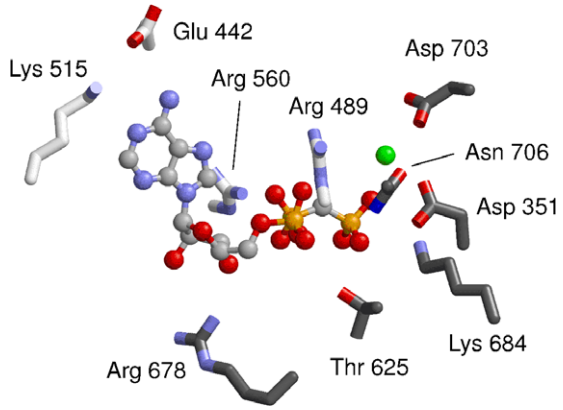

(b)

Fig. 1. (a) Structures of two ATPase states. Left: Ca_2E1 generated from pdb entry 1SU4; right: E2 stabilised by thapsigargin and 2,5-di-tert-butyl-1,4-dihydroxybenzene generated from pdb entry 2AGV [85]. The view is approximately parallel to the membrane surface. The approximate membrane boundaries as defined by Trp residues on the surface of the M domain are indicated by horizontal lines. Letters indicate domains. Colours in the web version of the article indicate Asp-351 (red), Ca^{2+} (bright green spheres), Na^+ (gold sphere) located at the K^+ binding site [179] and backbone regions that link the M domain with the cytoplasmic domains. Links between M and A domain: link containing M1 (orange), link containing M2 (dark red), link containing M3 (yellow). Links between M and P domain: M4 (blue), M5 (light blue), L67 (yellowish green). Backbone stretches with light colours are in front, those with dark colours in the back. Cyt stands for cytoplasm. (b) Binding of AMPPCP to the ATPase (pdb entry 1T5S [98]). The nucleotide is represented by balls and sticks, interacting amino acid side chains by sticks (for some residues only part of the side chain is shown). Carbon atoms of residues of the N domain are white, those of the P domain dark grey, the catalytic ion Mg^{2+} is green in the web version of the article. The figure was generated with RasTop.

as the E2 → E1 transition of the Ca^{2+} free enzyme [48,50,52]. Both models have been suggested to operate for different pools of the ATPase molecules [50]. Additionally, one [48] or two [43,54] protons modulate Ca^{2+} binding but do not compete directly with Ca^{2+}.

Ca^{2+} binding enables ATP to phosphorylate Asp-351 [5,6] of the ATPase which occludes the bound

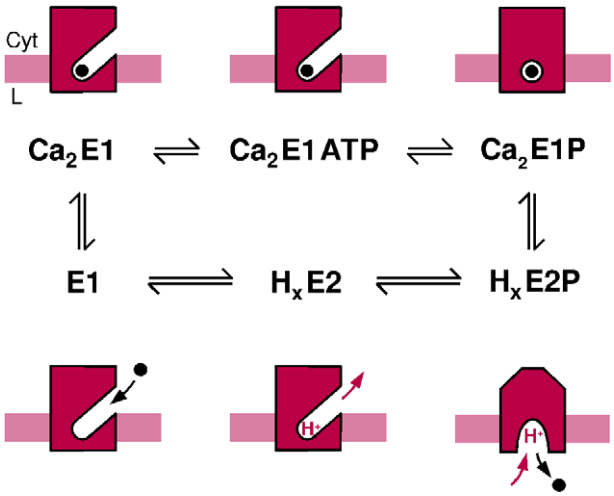

Fig. 2. Simplified reaction cycle of the Ca^{2+}-ATPase. The cartoons illustrate accessibility and protonation state of the Ca^{2+} binding sites. For clarity only one Ca^{2+} and one H^+ is indicated. Cyt stands for cytoplasm and L for lumen. The arrows indicate ion movements in the reaction step that follows the depicted state in the physiological progression of the reaction cycle (clockwise sense).

Ca^{2+} which makes Ca^{2+} dissociation to either side of the membrane very slow [11,55–57]. At least two phosphoenzyme intermediates (Ca_2E1P and E2P) with different properties [11,58–60] are formed consecutively [11,59,60]. The first phosphoenzyme intermediate Ca_2E1P is ADP-sensitive, i.e. dephosphorylates with ADP to form ATP. In the presence of a Ca^{2+} gradient, the Ca_2E1P phosphoenzyme can also hydrolyse (not shown in Fig. 2) without Ca^{2+} transport. This produces heat and likely contributes to maintaining body temperature [61].

The second phosphoenzyme intermediate E2P is ADP-insensitive (E2P) and dephosphorylates by reaction with water. The formation of E2P from Ca_2E1P is accompanied by release of Ca^{2+} into the SR lumen from Ca^{2+} sites with low affinity. Even high lumenal Ca^{2+} concentrations of up to 30 mM do not inhibit the lumenal release of Ca^{2+} from the phosphoenzyme [62,63]. Whether this Ca^{2+} release is sequential [45,64–66] or not [62,63] has been debated. Even when sequential dissociation is observed, the two Ca^{2+} seem to become mixed between binding and dissociation [67].

Departure of Ca^{2+} from its binding sites on the phosphoenzyme is accompanied by uptake of two to three H^+ from the SR lumen [52,53,68,69]. Protonation of protein residues of E2P has been found to decrease the affinity for Ca^{2+} [70,71] as well as to increase the stability of the phosphoenzyme against hydrolysis [72]. Hydrolysis of E2P [73] and regeneration of the high affinity Ca^{2+} binding sites complete the reaction cycle. All steps of the reaction cycle are reversible and ATP can be produced in the presence of a Ca^{2+} gradient or upon addition of Ca^{2+} to E2P [70,71,74,75].

1.4. Proton countertransport

Proton uptake and release reactions lead to proton countertransport. The stoichiometry of proton countertransport is two to three H^+ per two transported Ca^{2+} [51,52,69,76–78] making Ca^{2+} transport electrogenic [79]. Ca^{2+} and H^+ ions compete for the same sites of the Ca^{2+}-ATPase [49,53,77,80,81] where protons are supposed to be required for stabilisation of the ATPase structure by partly neutralizing the negative charge of the empty Ca^{2+} binding sites [28]. They bind up to four H^+ at low pH, which is

more than the number of transported H^+ [54]. Proton countertransport is pH dependent due to a pK_a of the cytoplasmic H^+ binding sites of approximately 5.8–6.1 [53,77] and a pK_a of the lumenal H^+ sites of 7.2–8.3 [52,53,77,82]. Consequently at pH 8, when binding of lumenal protons is reduced [77], the affinity of the Ca^{2+} binding sites is higher than at lower pH [65,83] and less Ca^{2+} is released towards the SR lumen [52].

The two Ca^{2+} binding sites contain four carboxyl groups, Glu-309 (Ca^{2+} binding site II), Glu-771 (site I), Asp-800 (sites I and II) and Glu-908 (site I) [20,84], which are thought to bind the countertransported protons according to electrostatic calculations [85–87] with possible exception of Glu-908 [85] and Glu-309 [87]. Mutagenesis studies have indicated a possible involvement of Glu-309 [88, 89], Glu-771 [90] and Asn-796 [91] in proton or H_3O^+ binding and proton countertransport. According to a recent suggestion, the proton path from the SR lumen to the acidic Ca^{2+} ligands is different from the Ca^{2+} exit path which enables rapid (partial) neutralisation of the empty Ca^{2+} binding sites [92].

1.5. Structural changes during Ca^{2+} transport

At present, crystal structures of most major transport intermediates or of their analogs are known [20,93–100]. The transition from Ca_2E1 to E2 or from Ca_2E1P to E2P disrupts the Ca^{2+} binding sites by rotation of coordinating residues of M6, movement of M4 towards the lumen [93,99,100], and the possibility for the Ca^{2+} ligand Glu-309 to orient away from the Ca^{2+} binding sites [87,93,94]. These movements seem to be unnecessarily large to promote Ca^{2+} dissociation but are explained by the relationship to the Na^+/K^+-ATPase which generates K^+ binding sites in this step [28,93].

Ca^{2+} binding and release to the phosphorylated and unphosphorylated ATPase are electrogenic [81] implying that the ions move through narrow channels [54]. Ca^{2+} channels have been proposed between M2, M4 and M6 [20,101] and between M1 and M2 for the Ca^{2+} bound state Ca_2E1 [30,98] and between M1 and M2 for the Ca^{2+} free state E2 [93]. No obvious Ca^{2+} exit pathway to the lumen has been found in the first structures of E2P analogs [94,96]. This is expected since the Ca^{2+} binding sites in these analogs are considerably less accessible than those of "true" E2P [41,94,102]. Nevertheless, two putative release pathways have been proposed: one between transmembrane helices M4 and M6 [96] and one between transmembrane helices M1, M2 and M4 [87]. The actual release pathway, seen in the recent structures of the BeF_3^- analog of E2P [99,100], is a "diplomatic compromise" between these suggestions: it runs between transmembrane helices M1, M2, M4, M5 and M6.

Structural changes during Ca^{2+} transport have recently been reviewed in detail [28,29,32] and will be summarised only briefly. The structure of Ca_2E1 shows an open arrangement of the three cytoplasmic domains with A and N domain loosely attached to the P domain, whereas they adopt a more compact conformation in all other intermediates (see Fig. 1(a)). However, the structure of Ca_2E1 might be less open, or that of E2 less closed under physiological conditions. The hinge between N and P domain is supposed to be flexible [19,103–105] which enables close approximation of the two domains when cross-linked by glutaraldehyde [106]. Fluorescence energy transfer experiments show that distances between fluorescence labels in the N- and the P-domain do not change between Ca_2E1 and an E2 conformation, as reviewed in [17]. Of particular interest is the unchanged distance between Cys-344 and Lys-515 [18, 107] and between Cys-344 and Glu-439 [18], in contrast to what is expected from the crystallographic models [20,93] as discussed previously [108].

Transmembrane helices M7 to M10 keep their position in the different transport intermediates and seem to anchor the protein in the membrane [28,94]. In contrast, transmembrane helices M1–M6 and the cytoplasmic domains A and N move considerably during Ca^{2+} transport (see Fig. 1(a)). The two domains

are connected via flexible linkers to the M and P domain, respectively, and interact non-covalently with the P domain. These interactions are modified during Ca^{2+} transport which repositions A and N domain with respect to the P domain without changing their internal structure [93,96,97]. The internal structure of the P domain is maintained upon Ca^{2+} binding [28] but its parallel β-sheet undergoes conformational changes upon ATP binding and dephosphorylation of E2P [97] enabled by its internal flexibility [105].

In order to coordinate events at the phosphorylation site and at the Ca^{2+} sites, structural changes within the P domain and movements of the entire domain have to be sensed by the M domain and vice versa. The two domains are structurally coupled in a direct way (i) by the long helices M4 and M5, which protrude into the P domain, (ii) by non-covalent interactions between P domain and M3 and (iii) via the loop between M6 and M7 (L67) which interacts with M5 [28,93,109] (see Fig. 1(a)). These interactions are thought to link movements of P and M domain [20,110–113] for example when M5 tilts and the P domain rotates with respect to the M domain upon Ca^{2+} binding.

A second important transmission path for the signalling between Ca^{2+} and phosphorylation sites is provided by the A domain, which indirectly links P and M domain. The A domain is connected to the M domain via M1–M3 (see Fig. 1(a)). Due to nucleotide binding and phosphorylation, the P domain provides different interaction surfaces in different intermediates, which makes the A domain bind in different orientations to the P domain, resulting in different "pulls" on the transmembrane helices and opening and closing of Ca^{2+} entry and exit paths [99,100]. Consequently, the length [40,114] and integrity [115,116] of these links are important for function.

2. Infrared difference spectroscopy

Infrared spectroscopy directly observes the backbone conformation of proteins and the functional groups of the amino acid side chains. Consequently, the intrinsic information content of the infrared spectrum is very high. Structure and interactions of molecular groups can be analysed and quantified in great detail. For example, small alterations can be detected to the strength of individual bonds (detection limit $<0.02\%$) [117], to bond lengths (<0.01 Å) [117], to the strength of hydrogen bonds (<2 kJ/mol, corresponding to 15% of a typical hydrogen bond) [117], and to protein backbone conformation (1 peptide group). For lipids, hydrogen bonding of the headgroups, acyl chain packing and acyl chain conformational order (number of *gauche* rotamers) can be investigated [118].

In time-resolved experiments it is possible to follow in the same experiment the kinetics of an overall backbone conformational change of the polypeptide backbone as well as the fate of single catalytically active groups, as for example the aspartylphosphate or the Ca^{2+} chelating groups. Thus infrared spectroscopy simultaneously looks, on the one hand, at highly specific local sites and, on the other hand, at the protein as a whole.

The difference in absorbance between two different protein states are usually very small, on the order of 0.1% of the maximum absorbance. Consequently, simply comparing the spectrum of a sample, where the protein is in state A, with a spectrum, where it is in state B, does usually not allow the sensitive detection of the small absorbance changes between the two protein states. Instead, the protein reaction of interest has to be initiated directly in the cuvette. To further complicate the experiment, the application of infrared spectroscopy to substrate-driven enzyme reactions is hindered by the strong water absorbance in the mid-infrared spectral range that requires an optical pathlength of 5–10 μm for H_2O solutions (30–50 μm for D_2O). Thus, adding the substrate to a protein sample is difficult. One of the approaches to overcome this problem is to release effector molecules via photolysis of biologically "silent" precursors (termed "caged compounds") as shown in Fig. 3 for the archetype of caged compounds, caged ATP

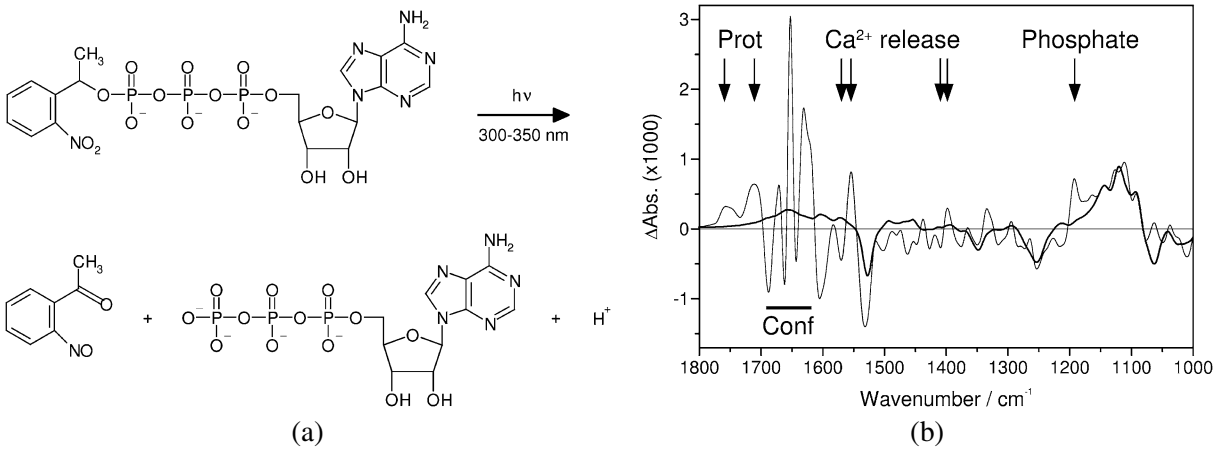

Fig. 3. Infrared difference spectroscopy with caged compounds at the example of caged ATP. (a) Photolysis of caged ATP. Caged ATP is modified at the γ-phosphate so that it does not react with the ATPase. Upon an UV flash (300–350 nm), the caged molecule photolyses which leads to a sudden concentration jump of free ATP ($<$10 ms). (b) Infrared difference spectra upon release of ATP from caged ATP. From a spectrum recorded before ATP release and spectra recorded after ATP release, difference spectra are calculated that originate only from those groups that are affected by ATP release. All "passive" residues are invisible in the difference spectrum which, therefore, exhibits details of the reaction mechanism on the molecular level despite a large background absorption. Negative bands in difference spectra are characteristic of the initial state before release of ATP, while positive bands reflect the state(s) after ATP release. In addition to protein and ATP bands, the photolysis reaction is reflected in the difference spectra. Thick line: spectrum of caged ATP photolysis in the absence of protein. The main bands at 1524 and 1342 cm^{-1} have been assigned to the antisymmetric and symmetric stretching vibrations of the nitro group of caged ATP, respectively, and below 1270 cm^{-1} to a diminution of electron density in the phosphate P–O bonds upon photolysis [125]. Further information can be found in [180–185]. Thin line: ATP release in a Ca^{2+}-ATPase sample. Two reactions contribute to the signals: (i) caged ATP photolysis and (ii) the transition of the Ca^{2+} loaded ATPase Ca_2E1 to the E2P phosphoenzyme where Ca^{2+} has been pumped and released. Tentative assignments of selected infrared difference bands are given. Prot: bands of protonated carboxyl groups due to protonation of acidic Ca^{2+} ligands upon Ca^{2+} release. The right and left band are characteristic of carbonyl groups with and without hydrogen bonding, respectively. Ca^{2+} release: bands of carboxylate groups due to Ca^{2+} release; Phosphate: band of the E2P phosphate group; Conf: bands predominantly due to conformational changes of the protein backbone. Reprinted in modified form from [186]. © 2002 American Chemical Society.

[119,120]. The sensitivity of this approach is high enough to detect environmental changes around single atoms in this 15,000 atom protein [121]. It is more sensitive than comparing absorbance spectra of different samples [122–124], which finds difficulty in detecting conformational changes between different ATPase states.

The Ca^{2+}-ATPase was the first protein to be studied by a photolytically induced concentration jump [125]. Caged ATP [38,125–127], other caged nucleotides [108,126] and the caged Ca^{2+} compounds Nitr 5 [128] and DM-Nitrophen [129,130] have been used. Early work [125–128] was done at low time resolution. It has established the conditions to obtain active ATPase samples for infrared spectroscopy with protein concentrations ($\sim$100 µg in 1 µl sample volume) nearly as high as those found in cells [131]. The sensitivity of infrared spectroscopy to a large number of chemical groups implies that the sample conditions can be controlled in the same experiment that monitors structural changes associated with ATPase reactions. For example, relative protein content [132], hydrolytic activity [125,126,133], and the amount of ATP released from caged ATP [126] can be quantified and reactions of other proteins present can be monitored [38,127,132].

To establish the functionality of the ATPase in the infrared samples, a number of control experiments have been employed: Ca^{2+} uptake upon ATP release in infrared films has been demonstrated with the

Ca^{2+} indicator Antipyrylazo III [126], the amplitude of infrared signals of a Ca^{2+} titration correlates with intrinsic fluorescence changes measured in the same samples [129], no significant infrared absorbance changes were observed upon ATP or Ca^{2+} release in control samples that contained ATPase inhibitors [127,128,130,134]; and upon nucleotide release in control samples containing 20 mM EGTA [126], which converts the ATPase to a Ca^{2+}-free state; or upon fluorescein isothiocyanate labeling of the ATPase [126], which blocks the ATP binding site [135,136].

The rapid scan technique has greatly improved the time resolution. With a time resolution of 65 ms, spectra of sequential states of the protein can be obtained as well as kinetic traces of individual difference bands that monitor environmental or structural changes of individual groups [38,130].

3. Detection of conformational changes

A first approach to the interpretation of infrared difference spectra is to regard them as a fingerprint of the underlying conformational change. In this way, the amplitude of the signals, their spectral shape and their kinetics can be analysed. Similar approaches have a long tradition in fluorescence spectroscopy, where "high" and "low" fluorescence have been used to define enzyme conformational states. Infrared spectroscopy has here the advantage of directly monitoring all peptide groups of a protein, therefore making a conformational change hard to miss. Of special interest is the absorbance of the amide I mode of the polypeptide backbone (predominantly a C=O vibration), in the region from 1700 to 1610 cm^{-1}, which is sensitive to secondary structure and hydrogen bonding to the backbone carbonyls.

From the magnitude of the difference signals in the amide I region of the spectrum, the extent of conformational change in a protein reaction may be estimated [38,130,137,138]. While this approach has several implications and limitations, as discussed previously [38,139,140], it nevertheless seems to provide realistic estimates of the *net* secondary structure change [139–141]. The *net* secondary structure change is very small and it has been concluded [38] from combining infrared and small angle X-ray diffraction data [142] that conformational changes in small flexible regions of the protein lead to significant movements of rigid protein domains relative to each other as later confirmed by X-ray crystallography.

From the infrared data, it does not seem possible to distinguish between minor and major secondary structure changes in the catalytic cycle of the Ca^{2+}-ATPase. This is in contrast to what would be expected from the classical model of the ATPase reaction cycle by de Meis and Vianna [33] that is based on only two main protein conformations E1 and E2, but is in line with the recent structural data. Instead, Ca^{2+} binding, ATP binding, phosphorylation and phosphoenzyme conversion are associated with secondary structure changes of comparable magnitude with that of phosphorylation somewhat smaller [38]. The clear detection of a conformational change upon phosphorylation is particularly interesting, because it is missed by X-ray crystallography [98]. This will be discussed further below. In addition, evidence has also been obtained for a pH dependent conformational change of the protein that affects the $Ca_2E1 \rightarrow E2P$ transition [82].

Difference spectra of the two Ca^{2+} release reactions from the phosphorylated ($Ca_2E1P \rightarrow E2P$) and the unphosphorylated enzyme ($Ca_2E1 \rightarrow E1/E2$) show striking similarity [143] and similar conformational changes have been concluded from this observation. Since difference spectra of a reaction contain information on protein structure, side chain protonation, hydrogen bonding and Ca^{2+} binding mode of the initial and the final state, the observed similarity suggests that the occupied and unoccupied Ca^{2+} binding sites are most likely the same in the two reactions. Thus, a model with only one pair of binding sites for Ca^{2+} is favoured from the infrared spectra. This is in contrast to the model by Jencks [144]

that proposes two different pairs of sites for cytoplasmic high affinity and lumenal low affinity binding sites, respectively. However, it is in agreement with mutagenesis studies [84] and with crystal structures in different ATPase states [93,96].

4. Protonation of the empty Ca^{2+} binding sites

Infrared bands of protonated Asp and Glu residues of E2P [126,132,145] and of Ca^{2+} free ATPase (E1 or E2) [128–130,143] have been observed upon Ca^{2+} release from the phosphoenzyme and Ca^{2+} binding to the unphosphorylated ATPase, respectively. These bands are marked with "prot" in Fig. 3(b) which shows a spectrum of E2P formation. The earlier suggestion that the bands of Ca^{2+} free ATPase are sensitive to the addition of dithiothreitol [128] could not be reproduced [129,130] and they have also been observed in the presence of glutathione [129]. Three of the E2P bands are pH dependent and titrate with a pK_a value near 8.3 [82] which is similar to the apparent pK_a value of residues binding lumenal H^+ for proton countertransport [52,53,77]. This similarity of the pK_a values supports the earlier interpretation that the bands originate from the protonation of carboxyl groups in the Ca^{2+} binding sites [129,130], which are involved in H^+ transport [143].

The spectral position of the bands indicates that some of the carboxyl carbonyl oxygens are hydrogen bonded while others are not. This observation has enabled a tentative assignment of the signals to Glu-771 (H-bonded), Asp-800 (some conformers H-bonded, some not) and Glu-908 (H-bonded) by multiconformation continuum electrostatics calculations [82]. The discussed bands of Ca^{2+} free ATPase and of E2P have the same spectral positions which has led to the proposal that the same amino acid residues become protonated in E1 or E2 as in E2P and that hydrogen bonding to the carbonyl oxygens is similar [143].

5. Nucleotide binding

5.1. Effect of individual interactions between ATP and ATPase on the structure of the nucleotide–ATPase complex

Binding of ATP induces conformational changes that are relatively large compared to those associated with the phosphorylation reaction as seen by infrared spectroscopy [38]. The largest absorbance changes upon binding have been observed for ATP, other nucleotides induce smaller changes. TNP-AMP binding to Ca_2E1 seems to cause small structural changes that are largely opposite to those induced by ATP [134]. Nucleotides which have individual functional groups of ATP modified produce nucleotide binding spectra that are different from the spectrum obtained with ATP as shown in Fig. 4. Therefore, the conformational change upon nucleotide binding depends to a surprising degree on individual interactions between ATPase and nucleotide [108,146].

The lack of individual interactions produces more than just local effects: it affects the entire conformational change upon binding. The effect is similar for modification at opposite ends of the ATP molecules which interact with different domains (N or P domain). In particular, omission of the γ-phosphate [146] and modification of the amino [108] group both reduce the conformational change, with the latter modification having a more dramatic effect. This suggests a concerted conformational change upon ATP binding for which all interactions need to be in place [108].

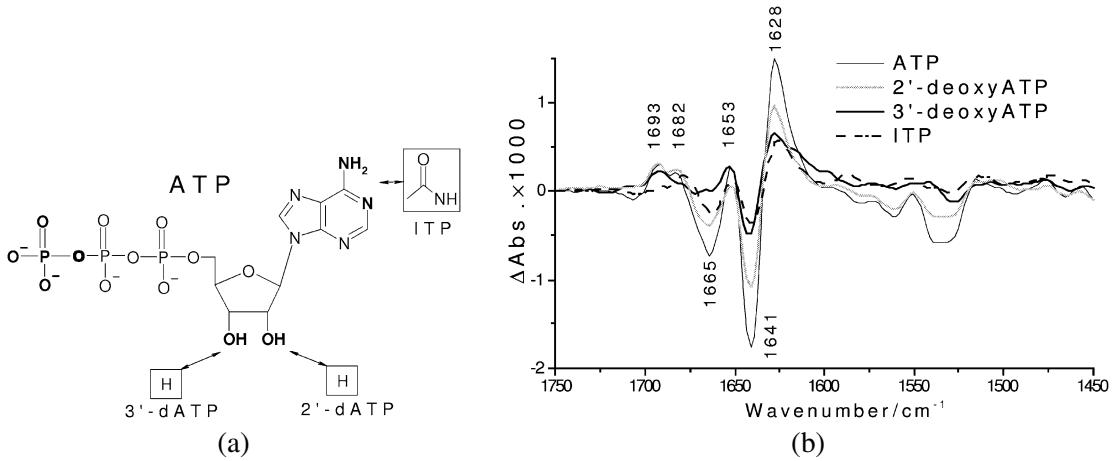

Fig. 4. Infrared absorbance changes induced by nucleotide binding to the ATPase. (a) Structures of ATP and ATP analogues highlighting the modified functional groups of ATP. (b) Difference spectra of nucleotide binding to the Ca^{2+}-ATPase ($Ca_2E1 \rightarrow Ca_2E1NTP$) obtained with ATP, 2′-deoxyATP, 3′-deoxyATP and ITP [108]. Labels indicate the band positions of the ATP binding spectrum. The difference spectra reflect conformational changes of the protein backbone in the amide I (1700–1610 cm^{-1}) region of the spectra: the positive signal near 1653 cm^{-1} is characteristic of α-helical structure, the signals near 1693, 1641 and 1628 cm^{-1} of β-sheets. Turn structures likely contribute to the signals near 1665 cm^{-1}. The spectra indicate that α-helices, β-sheets and turns are affected by nucleotide binding. Each modification of ATP affects the binding induced conformational change. Thus all groups modified are involved in important interactions with the ATPase. Reprinted in modified form from [140].

As a consequence of the sensitivity of the binding induced conformational change on individual interactions, the (average) structure of the nucleotide–ATPase complex is characteristic of the nucleotide bound. This explains some of the conflicting results obtained with different ATP analogs for the Ca^{2+}-ATPase and the Na^+/K^+-ATPase which has led to a controversy about the number of binding sites as summarised previously [147,148]. The finding of a nucleotide-specific conformation of the nucleotide–ATPase complexes is supported by previous reports, in which different effects of different nucleotides were found on fluorescence properties [149–151], partial reaction rates [152–155], protection against proteolysis [156], effects of aromatic compounds [157], nucleotide binding properties of mutants [158], and uncoupling [159].

From the infrared studies it has been concluded that the ATPase interacts with the γ-phosphate [146], the ribose hydroxyls and the amino function [108] of ATP. The interactions identified by infrared spectroscopy have later been confirmed by X-ray crystallography [97,98]. Figure 1(b) shows the nucleotide binding site with bound AMPPCP, which is a close ATP analog. The ribose 2′-OH interacts with Arg-678 and 3′-OH with Arg-560 and Arg-678. The position of Arg-678 is such that the 3′-OH hydrogen is directed towards the β-phosphate with which it forms a hydrogen bond that stabilises the unusual bent conformation of the phosphate chain. The amino group of adenine is close to Glu-442 and the γ-phosphate interacts with the P domain and stabilises a conformational change in this domain [97].

Binding of ATP closes a cleft between two of the cytoplasmic domains of the ATPase [28,29]: the nucleotide-binding domain (N domain) and the phosphorylation domain (P domain). Closure of the cleft delivers the γ-phosphate to the phosphorylation site Asp-351 in the P domain [97,98]. The two domains are bridged by ATP in Ca_2E1ATP which also provides an explanation for the drastic structural effects of modifying the ribose 3′-OH and the adenine amino function. Interactions of both groups stabilise the closed conformation of the complex, the 3′-OH group directly via an interaction with Arg-678 in the

P domain, and the amino group indirectly. Its interaction with Glu-442 of the N domain seems to position the ribose hydroxyls such that interaction with the P domain is possible. When ITP is used instead of ATP, Glu-442 will repell the negative partial charge on the inosine oxygen, reorient the inosine moiety and sacrifice interactions of the ribose hydroxyls with the P domain. This explains the weaker binding of ITP and the smaller extent of conformational change upon ITP binding [108].

What conformational changes are reflected in the infrared difference spectra? Movement of the A domain towards the P domain seems to contribute only slightly [108]. Rather the difference bands are caused [108,141] by the hinge movement between N and P domain [97,98] and the secondary hinge movement of the β-sheet in the P domain [98]. This movement aligns the β-sheet better in the ATP–ATPase complex and is thought to contribute to the main bands in the infrared difference spectra at 1641 and 1628 cm^{-1} [141].

5.2. β- and γ-phosphates interact as strong with the ATPase as with water

The results discussed so far in this chapter have been obtained by monitoring the conformational change of the peptide backbone. However, the absorption of the bound nucleotide can be observed directly if isotopic labeling is used to identify difference bands of specific nucleotide groups. Since the vibrational frequency depends on the masses of the vibrating atoms, isotopic labeling shifts the bands of labeled groups which can then be identified in the spectrum. In studies of nucleotide binding to the Ca^{2+}-ATPase, β- and γ-phosphates have been labeled and their infrared bands have been identified. They indicate that P–O bond strengths of the two phosphates are similar for ATP in aqueous solution and for bound ATP; i.e. that ATP's hydrogen bonds in aqueous solution are largely replaced by interactions with the protein for bound ATP [160]. In line with this, the β-phosphate interacts with Arg-560, ribose 3′-OH and likely with water in the crystal structures of Ca_2E1AMPPCP [97,98], as shown in Fig. 1(b). The γ-phosphate interacts with Mg^{2+}, Thr-625, Gly-626, Lys-684 and Asn-706.

5.3. Is AMPPCP a good ATP analog?

The X-ray structures of the ATP bound state Ca_2E1ATP [97,98] were obtained with the ATP analog AMPPCP instead of ATP. These structures are almost identical to the structures of a Ca_2E1P analog [96, 98]. In particular, in both states the side chain orientation of the Ca^{2+} ligand Glu-309 is largely [97], but not completely [87], locked and a putative Ca^{2+} access channel between transmembrane helices M1 and M2 is closed [98]. This similarity between the two structures obscures the structural cause for the functional difference between the ATP bound state and Ca_2E1P. In the ATP bound state, the Ca^{2+} ions are accessible whereas they are occluded in Ca_2E1P. A recent study has shed light on this paradox concluding that the Ca_2E1AMPPCP complex has different properties and structures at μM and mM Ca^{2+} concentration and resembles at low Ca^{2+} concentration more the ATP complex and at high Ca^{2+} concentration more Ca_2E1P [161]. In particular, Ca^{2+} dissociation is slowed down by AMPPCP at high but not at low Ca^{2+} concentrations. High Ca^{2+} concentration has been used to obtain the crystal structure of the AMPPCP complex [97] whereas most other studies have been done at lower Ca^{2+} concentration.

According to infrared spectroscopy, AMPPCP and AMPPNP are good analogs of ATP. The structure of the ATPase complex with ATP is very similar to those with AMPPCP [162] and AMPPNP [162,163] and all complexes seem to form a closed conformation of the cytoplasmic domains [162]. However, slight differences between the complex structure with ATP and that with the analogs are observed. The structure of one or several turns is more Ca_2E1P-like in the complex with ATP than in the complexes

with the ATP analogs AMPPCP and AMPPNP. The structure of a β-sheet, likely the β-sheet in the P domain, is similar for the AMPPCP and ATP complexes with Mg^{2+} as catalytic ion, but different with Ca^{2+}. This is likely caused by differences in ion coordination that affect the structure of the β-sheet in the P domain and which are further transmitted to the Ca^{2+} binding sites where they might affect Ca^{2+} dissociation as observed [161].

6. Phosphorylation

6.1. The structure of Ca_2E1P is similar but not identical to that of Ca_2E1ATP

Transfer of ATP's γ-phosphate to Asp-351 follows ATP binding. The crystal structures of the complex Ca_2E1AMPPCP and of the Ca_2E1P analogue Ca_2E1ADP: AlF^{4-} are almost identical and show a compact arrangement of domains [96,98]. In line with this, similar infrared spectra of ATP binding (Ca_2E1 $\rightarrow$ Ca_2E1ATP) and Ca_2E1P formation (Ca_2E1 $\rightarrow$ Ca_2E1P) [38] and similar proteolysis patterns [156] also indicate that the structures of Ca_2E1ATP and of Ca_2E1P are similar.

On the other hand, reaction rates of ATPase phosphorylation [164], changes in fluorescence levels [165,166], and infrared spectra [38,167] support the view that there is a conformational change in the reaction from the ATPase nucleotide complex to Ca_2E1P. It follows that the structures of the ATP–ATPase complex and that of the phosphoenzyme Ca_2E1P are similar but not identical.

6.2. Individual interactions between nucleotide and ATPase affect the phosphorylation reaction

Modifications at ATP's 2′-OH, 3′-OH and amino group affect phosphorylation of the Ca^{2+}-ATPase by modulating the change of protein structure and by slowing down the phosphorylation rate. Conformational changes upon phosphorylation are characteristic of the nucleotide used as shown by the different phosphorylation spectra obtained with different nucleotides [141]. This indicates that interactions of the ATP molecule distant from the phosphate groups contribute to approaching the γ-phosphate to the phosphorylation site Asp-351 and/or to forming the phosphate binding pocket. The functional groups 2′-OH, 3′-OH and the adenine ring of ATP are important for inducing the conformational change of the ATP–ATPase complex that is competent for phosphoryl transfer. Therefore, also phosphorylation is an interactive process in which the formation of interactions of the γ-phosphate is reinforced by interactions of other ATP groups, which can be at the opposite end of the ATP molecule. The infrared results point out the particular importance of the 3′-OH on enzyme phosphorylation. Its interaction with the protein seems to be a prerequisite for the closed conformation upon nucleotide binding [108] and for fast phosphorylation [141], in line with previous data [168].

An interesting feature observed with ITP are additional amide I signals in the phosphorylation spectrum as compared to ATP, which are similar to nucleotide binding signals [141]. Thus it seems that upon phosphorylation with ITP the enzyme catches up on a conformational change that has not been achieved by ITP binding because the interactions between protein and base moiety are impaired. In line with this result, an ATP-induced fluorescence change has not been observed for ITP binding but later for phosphorylation by ITP [151]. After dissociation of the diphosphate nucleotide from the phosphoenzyme, the structure of the phosphoenzyme is similar whether it has been generated by ATP, 2′ deoxy ATP or ITP.

6.3. Asp-351 interacts slightly stronger with Mg^{2+} than with Ca^{2+}

Bands of Ca_2E1P [132] and E2P [169] between 1708 and 1720 cm^{-1} have been assigned to the carbonyl group of phosphorylated Asp-351 based on model compound studies [167]. The band position of the putative Asp-351 band is sensitive to whether Mg^{2+} or Ca^{2+} is the catalytic ion that binds to the phosphorylation site [132,169]. This strengthens the assignment to Asp-351, since the putative carbonyl group of phosphorylated Asp-351 interacts with the catalytic ion in the crystal structures of Ca_2E1P analogs [96,98]. The C=O band of acetyl phosphate in aqueous solution [167] is observed very close to the respective bands of Ca_2E1P and E2P. This indicates similar strengths of the C=O bond and of the interactions between carbonyl oxygen and environment. From the spectral positions of the band it has been concluded that the Asp-351 C=O bond is weaker with Mg^{2+} than with Ca^{2+}, revealing a slightly stronger interaction between carbonyl oxygen and Mg^{2+}. The effect is more pronounced in E2P than in Ca_2E1P [169].

The band position of the aspartyl phosphate C=O group of Ca_2E1P is neither affected by the isotopic replacement of bulk H_2O by D_2O, nor by the addition of 20% Me_2SO, in contrast to the model compound acetyl phosphate in aqueous solution. This indicates that the C=O group does not interact with bulk water. In line with this, the bandwidth of the 1719 cm^{-1} band is significantly decreased compared to the bandwidth of acetyl phosphate which can be explained by a restricted freedom of conformation due to defined interactions of the C=O group with its environment [167].

7. ADP stabilises the closed conformation of the phosphoenzyme

ADP dissociation results in conformational changes which are the reverse of those induced by ADP binding to the ATPase [170]. This is indicated by infrared experiments that accumulate Ca_2E1P and in which ADP is removed by the helper enzyme apyrase. The extent of conformational change seems to be smaller when ADP dissociates from Ca_2E1P than when it binds to Ca_2E1. Upon dissociation of ADP from the phosphoenzyme, the conformation of Ca_2E1P relaxes partially back to that of the unphosphorylated state Ca_2E1. Thus, ADP plays an important role in stabilizing the closed conformation of Ca_2E1P [141,170]. ADP dissociation from Ca_2E1P is required for the transition to E2P in order to make room for the TGES motif of the A domain [94,96], but does not trigger the transition to E2P under conditions that favour Ca_2E1P (10 mM Ca^{2+} and 150 mM K^+) [170], since the infrared bands of E2P [38,132,145] are not observed upon ADP dissociation [170].

8. Phosphoenzyme phosphate group

8.1. The environment of the phosphoenzyme phosphate group controls Ca^{2+} pumping

The ATPase is one of the many examples in which phosphorylation controls biochemical reactions. The ATPase phosphoenzymes have different properties, which is essential for coupling ATP hydrolysis to Ca^{2+} transport [171]. For example, E2P dephosphorylates faster with water than Ca_2E1P and the model compound acetyl phosphate. This is required for the fast progression of the pump cycle and therefore for the efficient removal of Ca^{2+} from the cytoplasm of muscle cells. Obviously, the environment of the phosphate group is important in controlling the dephosphorylation properties. It has been found to become more hydrophobic in the transition from Ca_2E1P to E2P [70,172] and this seems to account

for an increased hydrolysis rate of E2P as compared to Ca_2E1P [173], reviewed in [174]. In addition, a water molecule is bound such that it can readily attack the phosphate group mainly by Thr-181 and Glu-183 of the A domain and also by Thr-625 and Gly-626 of the P domain [94,96].

8.2. The infrared absorption of the phosphoenzyme phosphate group can be detected

Bond properties and interactions of the phosphate group have been characterised by infrared spectroscopy. The essential step here is to identify the phosphate absorption in the difference spectra with help of isotopic substitution. Work on Ca_2E1P [160,167] and initial work on E2P [145] has compared infrared difference spectra obtained with labeled and unlabeled γ-phosphate of ATP. This approach has identified isotope-sensitive bands of Ca_2E1P and E2P which can be assigned to the phosphate group. The band positions are different for the two phosphoenzymes, indicating a conformational change that directly affects geometry and electron density of the phosphate group and makes the environment in E2P more hydrophobic [145].

The complete set of three E2P P–O stretching vibrations has been determined in an isotope exchange experiment which is more sensitive than the comparison of spectra obtained with different isotopes of ATP [121]. The experiment has observed an oxygen isotope exchange at the phosphate group that is catalysed by the ATPase [175]. It provides an infrared spectrum at "atomic resolution" in a crowded spectral region [121,176] which reveals the three stretching vibrations of the transiently bound phosphate group in spite of a background absorption of 50,000 protein vibrations. Bands of the terminal P–O stretching vibrations of the unlabeled phosphate group are found at 1194, 1137 and 1115 cm^{-1}. This isotope exchange experiment has not been possible for Ca_2E1P because this intermediate does not catalyse isotope exchange with water. Therefore the knowledge of the Ca_2E1P phosphate vibrations is less complete.

8.3. The protein environment modulates the bond properties of the phosphoenzyme phosphate group

The spectral positions of the absorbance bands of the phosphate group have been evaluated for Ca_2E1P [160,169] and E2P [176] using a correlation between P–O frequency and P–O bond valence, the bond valence model and empirical correlations to calculate P–O bond strengths, P–O bond lengths, and finally the dissociation energy of the bridging P–O bond [176]. Compared to the model compound acetyl phosphate, structure and charge distribution of the E2P aspartyl phosphate resemble somewhat the transition state in a dissociative phosphate transfer reaction: the aspartyl phosphate of E2P has 0.02 Å shorter terminal P–O bonds and a 0.09 Å longer bridging P–O bond, which is $\sim$20% weaker and has 64–90 kJ/mol less bond energy [176]. These findings are summarised in Fig. 5. Similar effects have been concluded for Ca_2E1P [160,169], the values of which are between those of acetyl phosphate and E2P, but closer to those of E2P. Interestingly, the differences between acetyl phosphate and the phosphoenzymes in the bridging P–O equilibrium bond length (max. 0.09 Å) are comparable to the bond length fluctuations in the vibrational ground state ($\pm$0.06 Å) [169].

8.4. The phosphate environment is not hydrophobic

The interactions between the terminal phosphate oxygens and protein in Ca_2E1P [169] and E2P [176] are $\sim$10% weaker than those of acetyl phosphate with water, indicating that the environment of the terminal phosphate oxygens is less hydrophilic as suggested previously [70,172–174]. However, the average interaction of each terminal phosphate oxygen is still considerable, being comparable to three

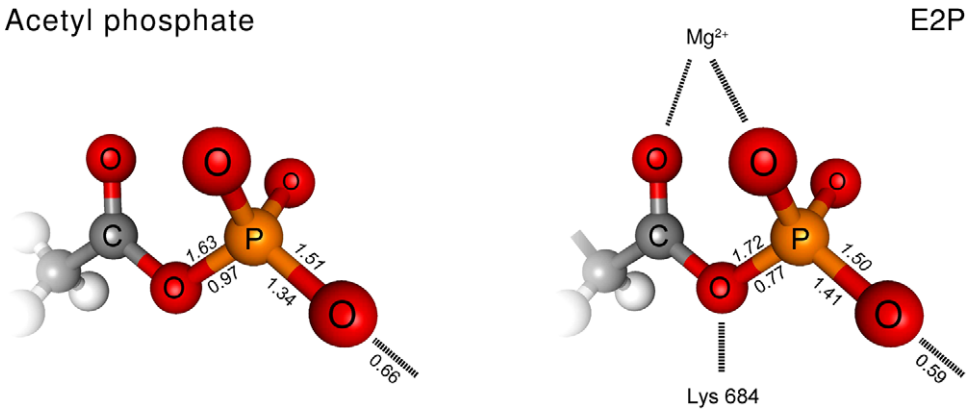

Fig. 5. Phosphate bond parameters for the model compound acetyl phosphate and E2P [176]. Italic numbers above bonds give bond lengths in Å, normal print numbers below bonds give bond valences in vu [187]. Reprinted in modified form from [140].

hydrogen bonds in ice [176]. Therefore, it is inappropriate to classify the environment of the phosphate group as hydrophobic.

8.5. What causes destabilisation of the bridging P–O bond?

The strength of the bridging P–O bond is determined by the relative strength of non-covalent bonding to the phosphate and aspartyl oxygens. The bridging P–O bond becomes weaker when the non-covalent interactions to the terminal phosphate oxygens become weaker and those to the aspartyl oxygens stronger [176]. In the case of the Ca^{2+}-ATPase phosphoenzymes, predominantly the bridging oxygen interacts stronger with its environment than acetyl phosphate in aqueous solution [169]. In line with the suggestion of strong interactions of the bridging oxygen with the protein environment, Lys-684 is close to the bridging oxygen in the crystal structures of Ca_2E1P and E2P analogs [94,96,98]. It is therefore a crucial residue, either initiating or compensating the shift of interactions from phosphate oxygens to the bridging oxygen.

There is an apparent contradiction between the P–O bond destabilisation and less external bonding to the phosphate group described above and the view that the phosphate group is stabilised on E2P [171]. The latter has been concluded from the observation that the free energy of the Ca^{2+} free enzyme plus phosphate and that of E2P are approximately the same, whereas that of acetyl phosphate is higher than that of acetate plus phosphate. From this, a stabilisation of E2P relative to acetyl phosphate has been concluded which is ascribed to the intrinsic binding energy of the phosphate moiety of the acyl phosphate when it binds to the active site [171].

This view concentrates on the phosphate group and ascribes a rather passive role to protein and solvent. In the presence of protein conformational changes and solvent exclusion there may be stabilising effects which are not localised on the phosphate group (but are caused by phosphorylation). Thus weaker bonding to the phosphate group may be overcompensated by stronger bonding between other groups and by entropic effects. One such effect is stronger bonding to the aspartyl moiety inferred from the infrared data.

8.6. Destabilisation of the bridging P–O is important for function

The strength of the bridging P–O bond is one of the key factors that tunes the hydrolysis rate of the ATPase phosphoenzymes and related phosphoproteins. The weaker bridging P–O bond of Ca_2E1P as compared to acetyl phosphate will reduce the activation energy required for bond breakage upon phosphate transfer which will be one cause for the fast transfer of the aspartyl phosphate to ADP [25, 177]. On the other hand, the bridging P–O bond of Ca_2E1P is stronger than that of E2P which will make the aspartyl phosphate of Ca_2E1P less susceptible to the "unwanted" attack by water [160].

The weaker bridging P–O bond of E2P with respect to acetyl phosphate in water accounts for a 10^{11}– 10^{15}-fold hydrolysis rate enhancement. Therefore, P–O bond destabilization is an important factor that facilitates phosphoenzyme hydrolysis [176].

8.7. What an elegant mechanism to control hydrolytic activity!

A weaker bridging P–O bond and stronger terminal P–O bonds are expected for a transition state in a dissociative phosphate transfer reaction. Thus, the bond strengths changes observed in going from aqueous environment to the Ca_2E1P and E2P environment of the phosphate group indicate that the enzyme environment prepares the phosphate group for a transfer reaction with dissociative character [169,176]. Recently, X-ray structures have been interpreted as giving evidence for strongly associative phosphate transfer reactions of both phosphoenzyme intermediates [94,98]. However, an evaluation [160] of the X-ray structures reveals that the transition states of Ca_2E1P and E2P have considerable associative and dissociative character, which is in agreement with the dissociative character inferred from our infrared experiments [160,176].

The destabilisation of the bridging P–O bond is a ground state property of Ca_2E1P and E2P. This finding is consistent with the view that part of the catalytic power of enzymes derives from ground state properties, in particular from favouring near-attack conformations in which the arrangement of reacting atoms is similar to that in the transition state [178].

The energy required to stretch the bridging acetyl phosphate P–O bond from its equilibrium bond length to the equilibrium lengths in Ca_2E1P and E2P is only 4 and 10 kJ/mol, respectively (2–4 times the thermal energy RT) [169]. This is far less than the differences in bond energy concluded from the infrared data, indicating that mechanical strain is an ineffective strategy to overcome the activation barrier of a dissociative phosphate transfer reaction. Therefore, weakening and elongation of the bridging P–O bond is not accomplished by external mechanical forces that pull the bond apart. More effective are environmental changes, the operating principle of the ATPase, which alter the equilibrium bond length and the bond energy [169]. This effect on bond properties is an in-built response of aspartyl phosphate to a shift of interactions from phosphate to aspartyl oxygens, with only subtle changes in distances required. Modulating these interactions provides an elegant "handle" for the enzyme to control its catalytic power.

Acknowledgements

The author gratefully acknowledges W. Hasselbach (Max-Planck-Institut, Heidelberg) for the gift of Ca^{2+}-ATPase, W. Mäntele (Johann Wolfgang Goethe-Universität, Frankfurt am Main) for his support in the early phase of the work described and J.E.T. Corrie (National Institute for Medical Research, London) for a fruitful collaboration on caged compounds. Work by the author has been supported by Deutsche Forschungsgemeinschaft, Vetenskapsrådet, Knut och Alice Wallenbergs Stiftelse, Carl Tryggers Stiftelse, Wenner-Grenska Samfundet and Wenner-Gren Stiftelserna.

References

[1] D.F.S. Rolfe and G.C. Brown, *Physiol. Rev.* **77** (1997), 731–758.
[2] W. Hasselbach and M. Makinose, *Biochem. Z.* **333** (1961), 518–528.
[3] K.B. Axelsen and M.G. Palmgren, *J. Mol. Evol.* **46** (1998), 84–101.
[4] W. Hasselbach and W. Waas, *Ann. N.Y. Acad. Sci.* **402** (1982), 459–469.
[5] D.H. MacLennan, C.J. Brandl, B. Korczak and N.M. Green, *Nature* **316** (1985), 696–700.
[6] C.J. Brandl, N.M. Green, B. Korczak and D.H. MacLennan, *Cell* **44** (1986), 597–607.
[7] D.W. Martin, C. Tanford and J.A. Reynolds, *Proc. Natl. Acad. Sci. USA* **81** (1984), 6623–6626.
[8] B. Vilsen and J.P. Andersen, *Biochim. Biophys. Acta* **855** (1986), 429–431.
[9] J.P. Andersen, P.L. Jorgensen and J.V. Moller, *Proc. Natl. Acad. Sci. USA* **82** (1985), 4573–4577.
[10] J.P. Andersen, K. Lassen and J.V. Moller, *J. Biol. Chem.* **260** (1985), 371–380.
[11] Y. Takakuwa and T. Kanazawa, *Biochem. Biophys. Res. Commun.* **88** (1979), 1209–1216.
[12] Y. Dupont, S.C. Harrison and W. Hasselbach, *Nature* **244** (1973), 555–558.
[13] L. Herbette, P. DeFoor, S. Fleischer, D. Pascolini, A. Scarpa and J.K. Blasie, *Biochim. Biophys. Acta* **817** (1985), 103–122.
[14] A.N. Martonosi, *Biosci. Rep.* **15** (1995), 263–281.
[15] C. Toyoshima, H. Sasabe and D.L. Stokes, *Nature* **362** (1993), 469–471.
[16] P. Zhang, C. Toyoshima, K. Yonekura, N.M. Green and D.L. Stokes, *Nature* **392** (1998), 835–839.
[17] D.J. Bigelow and G. Inesi, *Biochim. Biophys. Acta* **1113** (1992), 323–338.
[18] H.I. Stefanova, A.M. Mata, M.G. Gore, J.M. East and A.G. Lee, *Biochemistry* **32** (1993), 6095–6103.
[19] I. Jona, J. Matko and A. Martonosi, *Biochim. Biophys. Acta* **1028** (1990), 183–199.
[20] C. Toyoshima, M. Nakasako, H. Nomura and H. Ogawa, *Nature* **405** (2000), 647–655.
[21] D.M. Clarke, T.W. Loo, G. Inesi and D.H. MacLennan, *Nature* **339** (1989), 476–478.
[22] J.P. Andersen and B. Vilsen, *Acta Physiol. Scand.* **163** (1998), 45–54.
[23] A.N. Martonosi and S. Pikula, *Acta Biochim. Pol.* **50** (2003), 337–365.
[24] J.P. Andersen, *Biochim. Biophys. Acta* **988** (1989), 47–72.
[25] G. Inesi and L. de Meis, Kinetic regulation of catalytic and transport activities in sarcoplasmic reticulum ATPase, in: *The Enzymes of Biological Membranes*, 2nd edn, Vol. 3, A. Martonosi, ed., Plenum Press, New York, London, 1985, pp. 157–191.
[26] W. Hasselbach, *Top. Curr. Chem.* **78** (1979), 1–56.
[27] E. Mintz and F. Guillain, *Biochim. Biophys. Acta* **1318** (1997), 52–70.
[28] C. Toyoshima and G. Inesi, *Annu. Rev. Biochem.* **73** (2004), 269–292.
[29] D.L. Stokes and N.M. Green, *Annu. Rev. Biophys. Biomol. Struct.* **32** (2003), 445–468.
[30] A. Lee and J. East, *Biochem. J.* **356** (2001), 665–683.
[31] H.-J. Apell, *Bioelectrochemistry* **63** (2004), 149–156.
[32] J.V. Møller, P. Nissen, T.L.-M. Sørensen and M. le Maire, *Curr. Opin. Struct. Biol.* **15** (2005), 387–393.
[33] L. De Meis and A. Vianna, *Annu. Rev. Biochem.* **48** (1979), 275–292.
[34] D. Khananshvili and W.P. Jencks, *Biochemistry* **27** (1988), 2943–2952.
[35] N. Stahl and W.P. Jencks, *Biochemistry* **26** (1987), 7654–7667.
[36] J. Myung and W.P. Jencks, *Biochemistry* **34** (1995), 3077–3083.
[37] W.P. Jencks, T. Yang, D. Peisach and J. Myung, *Biochemistry* **32** (1993), 7030–7034.
[38] A. Barth, F. von Germar, W. Kreutz and W. Mäntele, *J. Biol. Chem.* **271** (1996), 30637–30646.
[39] S. Kato, M. Kamidochi, T. Daiho, K. Yamasaki, W. Gouli and H. Suzuki, *J. Biol. Chem.* **278** (2003), 9624–9629.
[40] T. Daiho, K. Yamasaki, S. Danko and H. Suzuki, *J. Biol. Chem.* **282** (2007), 34429–34447.
[41] M. Picard, C. Toyoshima and P. Champeil, *J. Biol. Chem.* **281** (2006), 3360–3369.
[42] U. Pick and S.J.D. Karlish, *J. Biol. Chem.* **257** (1982), 6120–6126.
[43] R.J. Froud and A.G. Lee, *Biochemistry* **237** (1986), 197–206.
[44] Y. Dupont, *Biochim. Biophys. Acta* **688** (1982), 75–87.
[45] G. Inesi, *J. Biol. Chem.* **262** (1987), 16338–16342.
[46] S. Orlowski and P. Champeil, *Biochemistry* **30** (1991), 352–361.
[47] C. Tanford, J.A. Reynolds and E.A. Johnson, *Proc. Natl. Acad. Sci. USA* **84** (1987), 7094–7098.
[48] V. Forge, E. Mintz and F. Guillain, *J. Biol. Chem.* **268** (1993), 10953–10960.
[49] R.B. Martin, *FEBS Lett.* **308** (1992), 59–61.
[50] J. Nakamura, *J. Biol. Chem.* **269** (1994), 30822–30827.
[51] M. Chiesi and G. Inesi, *Biochemistry* **19** (1980), 2912–2928.
[52] F. Tadini-Buoninsegni, G. Bartolommei, M.R. Moncelli, R. Guidelli and G. Inesi, *J. Biol. Chem.* **281** (2006), 37720–37727.

[53] C. Peinelt and H.-J. Apell, *Biophys. J.* **82** (2002), 170–181.
[54] A. Fibich, K. Janko and H.-J. Apell, *Biophys. J.* **93** (2007), 3092–3104.
[55] M. Sumida and Y. Tonomura, *J. Biochem.* **75** (1974), 283–297.
[56] S. Verjovski-Almeida, M. Kurzmack and G. Inesi, *Biochemistry* **17** (1978), 5006–5013.
[57] Y. Nakamura and Y. Tonomura, *J. Biochem.* **91** (1982), 449–461.
[58] F.U. Beil, D. von Chak and W. Hasselbach, *Eur. J. Biochem.* **81** (1977), 151–164.
[59] H. Takisawa and Y. Tonomura, *J. Biochem.* **86** (1979), 425–441.
[60] M. Shigekawa and J.P. Dougherty, *J. Biol. Chem.* **253** (1978), 1458–1464.
[61] L. de Meis, A.P. Arruda and D.P. Carvalho, *Biosci. Rep.* **25** (2005), 181–190.
[62] A.M. Hanel and W.P. Jencks, *Biochemistry* **30** (1991), 11320–11330.
[63] S. Orlowski and P. Champeil, *Biochemistry* **30** (1991), 11331–11342.
[64] J. Nakamura, *J. Biol. Chem.* **262** (1987), 14492–14497.
[65] V. Forge, E. Mintz, D. Canet and F. Guillain, *J. Biol. Chem.* **270** (1995), 18271–18276.
[66] R.C. Duggleby, J.M. East and A.G. Lee, *Biochem. J.* **339** (1999), 351–357.
[67] D. Canet, V. Forge, F. Guillain and E. Mintz, *J. Biol. Chem.* **271** (1996), 20566–20572.
[68] M. Yamaguchi and T. Kanazawa, *J. Biol. Chem.* **260** (1985), 4896–4900.
[69] F.T. Buoninsegni, G. Bartolommei, M.R. Moncelli, G. Inesi and R. Guidelli, *Biophys. J.* **86** (2004), 3671–3686.
[70] L. De Meis, O.B. Martins and E.W. Alves, *Biochemistry* **19** (1980), 4253–4261.
[71] L. De Meis and G. Inesi, *J. Biol. Chem.* **257** (1982), 1289–1294.
[72] G. Inesi, D. Lewis and A.J. Murphy, *J. Biol. Chem.* **259** (1984), 996–1003.
[73] M. Makinose, *FEBS Lett.* **37** (1973), 140–143.
[74] M. Makinose, *FEBS Lett.* **12** (1971), 269–270.
[75] W. Hasselbach, *Biochim. Biophys. Acta* **515** (1978), 23–53.
[76] D. Levy, M. Seigneuret, A. Bluzat and J.L. Rigaud, *J. Biol. Chem.* **265** (1990), 19524–19534.
[77] X. Yu, L.N. Hao and G. Inesi, *J. Biol. Chem.* **269** (1994), 16656–16661.
[78] X. Yu, S. Carrol, J.-L. Rigaud and G. Inesi, *Biophys. J.* **64** (1993), 1232–1242.
[79] K. Hartung, E. Grell, W. Hasselbach and W. Bamberg, *Biochim. Biophys. Acta* **900** (1987), 209–220.
[80] G. Inesi and T.L. Hill, *Biophys. J.* **44** (1983), 271–280.
[81] C. Butscher, M. Roudna and H.J. Apell, *J. Membr. Biol.* **168** (1999), 169–181.
[82] J. Andersson, K. Hauser, E.-L. Karjalainen and A. Barth, *Biophys. J.* **94** (2008), 600–611.
[83] S. Verjovski-Almeida and L. De Meis, *Biochemistry* **16** (1977), 329–334.
[84] J.P. Andersen, *Biosci. Rep.* **15** (1995), 243–261.
[85] K. Obara, N. Miyashita, C. Xu, I. Toyoshima, Y. Sugita, G. Inesi and C. Toyoshima, *Proc. Natl. Acad. Sci. USA* **102** (2005), 14489–14496.
[86] K. Hauser, *Biopolymers* **82** (2006), 430–434.
[87] K. Hauser and A. Barth, *Biophys. J.* **93** (2007), 3259–3270.
[88] B. Vilsen and J.P. Andersen, *FEBS Lett.* **306** (1992), 247–250.
[89] B. Vilsen and J.P. Andersen, *Biochemistry* **37** (1998), 10961–10971.
[90] J.P. Andersen, *FEBS Lett.* **354** (1994), 93–96.
[91] J.P. Andersen and B. Vilsen, *J. Biol. Chem.* **269** (1994), 15931–15936.
[92] E.-L. Karjalainen, K. Hauser and A. Barth, *Biochim. Biophys. Acta* **1767** (2007), 1310–1318.
[93] C. Toyoshima and H. Nomura, *Nature* **418** (2002), 605–611.
[94] C. Olesen, T.L.-M. Sørensen, R.C. Nielsen, J.V. Møller and P. Nissen, *Science* **306** (2004), 2251–2255.
[95] A.M.L. Jensen, T.L.M. Sørensen, C. Olesen, J.V. Møller and P. Nissen, *EMBO J.* **25** (2006), 2305–2314.
[96] C. Toyoshima, H. Nomura and T. Tsuda, *Nature* **432** (2004), 361–368.
[97] C. Toyoshima and T. Mizutani, *Nature* **430** (2004), 529–535.
[98] T.L.-M. Sørensen, J.V. Møller and P. Nissen, *Science* **304** (2004), 1672–1675.
[99] C. Olesen, M. Picard, A.-M.L. Winther, C. Gyrup, J.P. Morth, C. Oxvig, J.V. Møller and P. Nissen, *Nature* **450** (2007), 1036–1042.
[100] C. Toyoshima, Y. Norimatsu, S. Iwasawa, T. Tsuda and H. Ogawa, *Proc. Natl. Acad. Sci. USA* **104** (2007), 19831–19836.
[101] V. Costa and P. Carloni, *Proteins* **50** (2003), 104–113.
[102] S. Danko, K. Yamasaki, T. Daiho and H. Suzuki, *J. Biol. Chem.* **279** (2004), 14991–14998.
[103] S. Huang and T.C. Squier, *Biochemistry* **37** (1998), 18064–18073.
[104] C. Xu, W.J. Rice, W. He and D.L. Stokes, *J. Mol. Biol.* **316** (2002), 201–211.
[105] N. Reuter, K. Hinsen and J.J. Lacapere, *Biophys. J.* **85** (2003), 2186–2197.
[106] D.B. McIntosh, *J. Biol. Chem.* **267** (1992), 22328–22335.
[107] A.M. Mata, H.I. Stefanova, M.G. Gore, Y.M. Khan, J.M. East and A.G. Lee, *Biochim. Biophys. Acta* **1147** (1993), 6–12.
[108] M. Liu and A. Barth, *J. Biol. Chem.* **278** (2003), 10112–10118.

[109] A.G. Lee, *Biochim. Biophys. Acta* **1565** (2002), 246–266.
[110] T. Menguy, F. Corre, L. Bouneau, S. Deschamps, J.V. Møller, P. Champeil, M. le Maire and P. Falson, *J. Biol. Chem.* **273** (1998), 20134–20143.
[111] J.D. Clausen and J.P. Andersen, *J. Biol. Chem.* **279** (2004), 54426–54437.
[112] Z. Zhang, D. Lewis, C. Sumbilla, G. Inesi and C. Toyoshima, *J. Biol. Chem.* **276** (2001), 15232–15239.
[113] G. Lenoir, M. Picard, J.V. Møller, M. le Maire, P. Champeil and P. Falson, *J. Biol. Chem.* **279** (2004), 32125–32133.
[114] T. Daiho, K. Yamasaki, G. Wang, S. Danko, H. Iizuka and H. Suzuki, *J. Biol. Chem.* **278** (2003), 39197–39204.
[115] J.V. Møller, G. Lenoir, C. Marchand, C. Montigny, M. le Maire, C. Toyoshima, B.S. Juul and P. Champeil, *J. Biol. Chem.* **277** (2002), 38647–38659.
[116] G. Lenoir, M. Picard, C. Gauron, C. Montigny, P. le Marechal, P. Falson, M. le Maire, J.V. Møller and P. Champeil, *J. Biol. Chem.* **279** (2004), 9156–9166.
[117] H. Deng and R. Callender, *Methods Enzymol.* **308** (1999), 176–201.
[118] H.H. Mantsch, *J. Mol. Struct.* **113** (1984), 201–212.
[119] J.H. Kaplan, B. Forbush and J.F. Hoffman, *Biochemistry* **17** (1978), 1929–1935.
[120] J.A. McCray, L. Herbette, T. Kihara and D.R. Trentham, *Proc. Natl. Acad. Sci. USA* **77** (1980), 7237–7241.
[121] A. Barth, *Biopolymers (Biospectroscopy)* **67** (2002), 237–241.
[122] J. Villalain, J.C. Gomez-Fernandez, M. Jackson and D. Chapman, *Biochim. Biophys. Acta* **978** (1989), 305–312.
[123] J.L.R. Arrondo, H.H. Mantsch, N. Mullner, S. Pikula and A. Martonosi, *J. Biol. Chem.* **262** (1987), 9037–9043.
[124] R. Buchet, D. Carrier, P.T.T. Wong, I. Jona and A. Martonosi, *Biochim. Biophys. Acta* **1023** (1990), 107–118.
[125] A. Barth, W. Mäntele and W. Kreutz, *FEBS Lett.* **277** (1990), 147–150.
[126] A. Barth, W. Mäntele and W. Kreutz, *Biochim. Biophys. Acta* **1057** (1991), 115–123.
[127] R. Buchet, I. Jona and A. Martonosi, *Biochim. Biophys. Acta* **1104** (1992), 207–214.
[128] R. Buchet, I. Jona and A. Martonosi, *Biochim. Biophys. Acta* **1069** (1991), 209–217.
[129] H. Georg, A. Barth, W. Kreutz, F. Siebert and W. Mäntele, *Biochim. Biophys. Acta* **1188** (1994), 139–150.
[130] A. Troullier, K. Gerwert and Y. Dupont, *Biophys. J.* **71** (1996), 2970–2983.
[131] R.J. Ellis, *Curr. Opin. Struct. Biol.* **11** (2001), 114–119.
[132] A. Barth, W. Kreutz and W. Mäntele, *Biochim. Biophys. Acta* **1194** (1994), 75–91.
[133] D. Thoenges and A. Barth, *J. Biomol. Screen.* **7** (2002), 353–357.
[134] M. Liu and A. Barth, *Biophys. J.* **85** (2003), 3262–3270.
[135] U. Pick and S. Bassilian, *FEBS Lett.* **123** (1981), 127–130.
[136] S. Highsmith, *Biochem. Biophys. Res. Commun.* **124** (1984), 183–189.
[137] R.S. Chittock, S. Ward, A.-S. Wilkinson, P. Caspers, B. Mensch, M.G.P. Page and C.W. Wharton, *Biochem. J.* **338** (1999), 153–159.
[138] F. Scheirlinckx, R. Buchet, J.-M. Ruysschaert and E. Goormaghtigh, *Eur. J. Biochem.* **268** (2001), 3644–3653.
[139] A. Barth and C. Zscherp, *Quart. Rev. Biophys.* **35** (2002), 369–430.
[140] A. Barth, Infrared spectroscopy, in: *Methods in Protein Structure and Stability Analysis: Vibrational Spectroscopy*, V.N. Uversky and E.A. Permyakov, eds, Nova Science Publishers, New York, 2007, pp. 69–151.
[141] M. Liu and A. Barth, *J. Biol. Chem.* **279** (2004), 49902–49909.
[142] J.K. Blasie, L.G. Herbette, D. Pascolini, V. Skita, D.H. Pierce and A. Scarpa, *Biophys. J.* **48** (1985), 9–18.
[143] A. Barth, W. Mäntele and W. Kreutz, *J. Biol. Chem.* **272** (1997), 25507–25510.
[144] W.P. Jencks, *Biosci. Rep.* **15** (1995), 283–287.
[145] A. Barth, *J. Biol. Chem.* **274** (1999), 22170–22175.
[146] M. Liu and A. Barth, *Biopolymers (Biospectroscopy)* **67** (2002), 267–270.
[147] D.L. Stokes and N.M. Green, *Biophys. J.* **78** (2000), 1765–1776.
[148] D.B. McIntosh, *Adv. Mol. Cell Biol.* **23A** (1998), 33–99.
[149] J.-J. Lacapere, N. Bennett, Y. Dupont and F. Guillain, *J. Biol. Chem.* **265** (1990), 348–353.
[150] S. Wakabayashi and M. Shigekawa, *Biochemistry* **29** (1990), 7309–7318.
[151] K. Kubo, H. Suzuki and T. Kanazawa, *Biochim. Biophys. Acta* **1040** (1990), 251–259.
[152] P. Champeil, S. Riollet, S. Orlowski, F. Guillain, C.J. Seebregts and D.B. McIntosh, *J. Biol. Chem.* **263** (1988), 12288–12294.
[153] A.S. Hobbs, R.W. Albers, J.P. Froehlich and P.F. Heller, *J. Biol. Chem.* **260** (1985), 2035–2057.
[154] S.T. Ferreira and S. Verjovski-Almeida, *J. Biol. Chem.* **263** (1988), 9973–9980.
[155] H.M. Scofano, A. Vieyra and L. De Meis, *J. Biol. Chem.* **254** (1979), 10227–10231.
[156] S. Danko, K. Yamasaki, T. Daiho, H. Suzuki and C. Toyoshima, *FEBS Lett.* **505** (2001), 129–134.
[157] J.H. Petretski, H. Wolosker and L. De Meis, *J. Biol. Chem.* **264** (1989), 20339–20343.
[158] D.B. McIntosh, D.G. Woolley, D.H. MacLennan, B. Vilsen and J.P. Andersen, *J. Biol. Chem.* **274** (1999), 25227–25236.
[159] M.I. Fortea, F. Soler and F. Fernandez-Belda, *J. Biol. Chem.* **275** (2000), 12521–12529.
[160] M. Liu, M. Krasteva and A. Barth, *Biophys. J.* **89** (2005), 4352–4363.

[161] M. Picard, C. Toyoshima and P. Champeil, *J. Biol. Chem.* **280** (2005), 18745–18754.
[162] M. Krasteva and A. Barth, *Biochim. Biophys. Acta* **1767** (2007), 114–123.
[163] F. Von Germar, A. Barth and W. Mäntele, *Biophys. J.* **78** (2000), 1531–1540.
[164] J.R. Petithory and W.P. Jencks, *Biochemistry* **25** (1986), 4493–4497.
[165] H. Suzuki, S. Nakamura and T. Kanazawa, *Biochemistry* **33** (1994), 8240–8246.
[166] S. Nakamura, H. Suzuki and T. Kanazawa, *J. Biol. Chem.* **269** (1994), 16015–16019.
[167] A. Barth and W. Mäntele, *Biophys. J.* **75** (1998), 538–544.
[168] C. Coan, J.A. Amaral and S. Verjovski-Almeida, *J. Biol. Chem.* **268** (1993), 6917–6924.
[169] J. Andersson and A. Barth, *Biopolymers* **82** (2006), 353–357.
[170] M. Liu, E.-L. Karjalainen and A. Barth, *Biophys. J.* **88** (2005), 3615–3624.
[171] W.P. Jencks, *Methods Enzymol.* **171** (1989), 145–164.
[172] Y. Dupont and R. Pougeois, *FEBS Lett.* **156** (1983), 93–98.
[173] L. De Meis and V.A. Suzano, *FEBS Lett.* **232** (1988), 73–77.
[174] L. De Meis, *Biochim. Biophys. Acta* **973** (1989), 333–349.
[175] T. Kanazawa and P.D. Boyer, *J. Biol. Chem.* **248** (1973), 3163–3172.
[176] A. Barth and N. Bezlyepkina, *J. Biol. Chem.* **279** (2004), 51888–51896.
[177] C.M. Pickart and W.P. Jencks, *J. Biol. Chem.* **259** (1984), 1629–1643.
[178] T.C. Bruice and F.C. Lightstone, *Acc. Chem. Res.* **32** (1999), 127–136.
[179] T.L.M. Sørensen, J.D. Clausen, A.M.L. Jensen, B. Vilsen, J.V. Møller, J.P. Andersen and P. Nissen, *J. Biol. Chem.* **279** (2004), 46355–46358.
[180] A. Barth, K. Hauser, W. Mäntele, J.E.T. Corrie and D.R. Trentham, *J. Am. Chem. Soc.* **117** (1995), 10311–10316.
[181] A. Barth, J.E.T. Corrie, M.J. Gradwell, Y. Maeda, W. Mäntele, T. Meier and D.R. Trentham, *J. Am. Chem. Soc.* **119** (1997), 4149–4159.
[182] V. Cepus, C. Ulbrich, C. Allin, A. Troullier and K. Gerwert, *Methods Enzymol.* **291** (1998), 223–245.
[183] A. Barth, Time-resolved IR spectroscopy with caged compounds: An introduction, in: *Dynamic Studies in Biology: Phototriggers, Photoswitches and Caged Biomolecules*, M. Goeldner and R.S. Givens, eds, Wiley-VCH, Weinheim, 2005, pp. 369–399.
[184] V. Jayaraman, IR spectroscopy with caged compounds: Selected applications, in: *Dynamic Studies in Biology: Phototriggers, Photoswitches and Caged Biomolecules*, M. Goeldner and R.S. Givens, eds, Wiley-VCH, Weinheim, 2005, pp. 400–410.
[185] A. Barth and C. Zscherp, *FEBS Lett.* **477** (2000), 151–156.
[186] C. Zscherp and A. Barth, *Biochemistry* **40** (2001), 1875–1883.
[187] I.D. Brown, *The Chemical Bond in Inorganic Chemistry. The Bond Valence Model*, Oxford University Press, Oxford, 2002.